Preparation of Colloidal Nanoparticles of Mixed Metal Oxides Containing Platinum, Ruthenium, Osmium, and Iridium and Their Use as Electrocatalysts†

Manfred T. Reetz,*,‡ Marco Lopez,‡ Wolfgang Grünert,§ Walter Vogel,|| and Falko Mahlendorf⊥

Max-Planck-Institut für Kohlenforschung, Kaiser-Wilhelm-Platz 1, 45470 Mülheim/Ruhr, Germany, Ruhr-Universität Bochum, Universitätsstrasse 150, 44801 Bochum, Germany, Fritz-Haber-Institut der Max-Planck-Gesellschaft, Faradayweg 4−6, 14195 Berlin, Germany, and Universität Duisburg-Essen, Lotharstrasse 1-21, 47057 Duisburg, Germany

Received: December 20, 2002

The hydrolysis of H_2PtCl_6, $RuCl_3$, $OsCl_3$, and H_2IrCl_6 under basic conditions in the presence of a water-soluble betaine stabilizer affords aqueous colloidal solutions of the mixed metal oxide $PtRuOsIrO_x$ displaying a particle size of 1.3−1.6 nm. The ratio of the four metals can be adjusted by choosing the appropriate relative amounts of metal salts. Characterization was accomplished by TEM, XPS, and XRD. Immobilization of the reduced form on high surface conducting carbon leads to materials which are excellent electrocatalysts showing unusually high resistance to CO poisoning.

Introduction

A great deal of recent research has centered around the development of new methods for the preparation of nanosized transition metal colloids.[1] The most common methods involve the reduction of appropriate metal salts(s) in the presence of stabilizers such as polymers, surfactants, or special ligands which prevent undesired formation of insoluble bulk metal. Less is known concerning the respective metal oxides in the form of colloidal nanosized particles.[2] We have previously shown that treatment of $PtCl_4$ (or H_2PtCl_6) with such bases as NaOH, Na_2CO_3, or Li_2CO_3 in the presence of water-soluble betaine stabilizers of the type $R(CH_3)_2N^+(CH_2)_3SO_3^-$ results in the formation of stable aqueous solutions of colloidal PtO_2 having a particle size of 1.8 nm.[3] Moreover, upon using mixtures of $PtCl_4$ and $RuCl_3$, the colloidal mixed metal oxide $PtRuO_x$ was obtained, likewise as a stable aqueous solution of nanoparticles. It should be mentioned that $PtRuO_x$ is a simplified short-hand way of describing materials of this kind. In actual fact the colloid also contains hydroxy−metal moieties, certainly on the surface. These readily accessible colloids can be immobilized on solid supports and are thus attractive precursors for chemical and electrochemical catalysts.[3] For example, a potential field of application is electrocatalysis in direct methanol fuel cells (DMFCs) and polymer electrolyte fuel cells (PEFCs). If necessary, the metal oxide particles can be reduced to the zerovalent form by treatment with hydrogen either in the aqueous colloidal form or following immobilization on a solid support.[3] The actual synthesis involves base-catalyzed hydrolysis of the transition metal salts with concomitant condensation and cross-linking. The water-soluble betaine stabilizer prevents particle agglomeration and undesired precipitation of bulk metal oxide. The method is cheap and industrially viable because it avoids the use of organic solvents and does not require exceedingly large amounts of stabilizer.

In continuation of this research, we addressed the question whether more than two metals can be incorporated in the mixed metal oxide.[4] Specifically, we wanted to apply our synthetic method in order to prepare a mixed metal oxide comprising platinum, ruthenium, osmium, and iridium, namely, colloidal $PtRuOsIrO_x$ in water.[4] This particular combination was of specific interest because Smotkin and Mallouk had previously shown that quaternary alloys composed of Pt, Ru, Os, and Ir display promising electrocatalytic properties.[5] In their combinatorial electrochemical search, they prepared a variety of materials by $NaBH_4$-induced reduction of mixtures of metal salts, the proper combination of H_2PtCl_6, $RuCl_3$, $OsCl_3$, and K_2IrCl_6 leading to an insoluble material characterized as Pt(44)/Ru(41)/Os(10)/Ir(5) which was particularly effective as an anode catalyst in DMFCs with improved tolerance with respect to poisoning by CO. Later this material and similar compositions were prepared by arc-melting pressed pellets of Pt, Ru, Os, and Ir powders.[6] In the present paper, we show that our synthetic method can indeed be applied successfully to the preparation of colloidal nanosized $PtRuOsIrO_x$ in water. The study includes the characterization of this unusual mixed metal oxide, its reduction, and its use as an electrocatalyst.[4]

Experimental Section

Typical Procedure for the Preparation of $PtRuOsIrO_x$ Colloids. The commercially available (Fluka) betaine stabilizer 3-(*N*,*N*-dimethyldodecylammonio)propane sulfonate is dissolved in ultra-high-quality (UHQ) water so as to produce a 0.1 M solution. About 15 mL of this solution is placed in a clean 100 mL two-necked flask with 15 mL UHQ water containing 1.5 mmol of a base such as Li_2CO_3. Then 0.125 mmol of H_2PtCl_6 in 5 mL of UHQ water is added at room temperature with stirring. The other salts $RuCl_3$, $OsCl_3$, and H_2IrCl_6, each dissolved in 5 mL of UHQ water, are added in rapid succession with stirring, and the mixture is stirred at 60°C for 4−5 h. The pH of the solution should remain between 9 and 10, which can

† Part of the special issue "Arnim Henglein Festschrift".
* Corresponding author.
‡ Max-Planck-Institut für Kohlenforschung.
§ Ruhr-Universität Bochum.
|| Fritz-Haber-Institut der Max-Planck-Gesellschaft.
⊥ Universität Duisburg-Essen.

10.1021/jp027785a CCC: $25.00
Published on Web 07/10/2003

be accomplished by the addition of a saturated aqueous solution of Li_2CO_3. The reaction can be monitored by UV/vis spectroscopy, since the absorption of the Pt(IV) salt at 260 nm is gradually replaced by an unstructured plasmon band extending from 200 to 400 nm. Should a small amount of sedimentation occur, filtration (P4-frit) will be carried out. To remove ions from the black colloidal solution, standard dialysis with about 250 mL of deionized water is carried out twice for 20 h and then for 6 h with deionized water. HRTEM analysis (HF-7500 TEM instrument at 100 kV from Hitachi) shows the presence of 1.3 ± 0.4 nm sized particles. Freeze-drying provides a black solid that shows an elemental analysis (Mikroanalytisches Laboratorium H. Kolbe, Mülheim, Germany) corresponding to Pt(27)/Ru(20)/Os(23)/Ir(30). The solid can be redispersed in UHQ water (optionally in an ultrasonic bath to speed up dissolution), and TEM analysis points to the same nanoparticle size. Using different ratios of the salts leads to the corresponding (predictable) metal composition (see text below).

Typical Procedure for Reduction and Immobilization. The as above described prepared colloidal solution is treated with excess H_2 at room temperature for 24 h. An amount of high surface area conducting carbon (Vulcan XC 72) sufficient to yield the desired loading (e.g., 20% metal) is placed under argon in a three-necked 250 mL flask carrying a dropping funnel and a reflux condenser. It is evacuated and filled once more with argon. Then aqueous 0.1 M citrate buffer (pH 3.5, 40% of total volume) and UHQ water (20% total volume) are added, and the mixture is heated to 60°C. The colloidal solution is then added dropwise with stirring, and the suspension is stirred additionally for 40 h at 60°C and 18 h under reflux. The suspension is concentrated to dryness in a rotary evaporator and then treated with methanol (80 mL). The suspension is centrifuged for 20 min (6000 r/min), washed and centrifuged twice with methanol/water (2:1) and with methanol again, and centrifuged again. The moist solid is placed in a flask which is then dried in a vacuum for 24 h.

XPS Measurements. X-ray photoelectron spectra of the samples were recorded with a Leybold LHS 10 spectrometer equipped with a EA 10/100 multichannel detector (Specs). AlKα radiation (1483.6 eV, 12 kV * 20 mA) was used for excitation, and the data were measured with the analyzer at constant pass energy of 35.5 eV. The binding-energy (BE) scale was calibrated relative to C (1s) = 284.5 eV. The 4f lines of Pt, Ir, and Os were recorded together with the C (1s) line of the stabilizer. Due to the superposition of the latter with the main Ru signal (Ru (3d)), the Ru (3p) line was analyzed instead. The N (1s), O (1s), and S (2p) lines of the stabilizer were also included, but the results will not be reported in detail. Data reduction was performed with the software MacFit,[7] which permits the use of optimized parameters in the satellite subtraction routine. A highly accurate satellite subtraction, which has been employed elsewhere to decrease the detection level for vanadium oxide materials,[8] is essential for the reliable analysis of small Ir amounts, the Ir 4f signal of which would interfere with the X-ray satellites of the Pt 4f line (see below). Due to a sample damage problem (see below), the analysis of the spectral shapes had to be performed with data containing considerable experimental noise. The intensities were, however, evaluated from spectra after long acquisition time; therefore, the accuracy of the quantitative analyses given is estimated to be ±10% (rel) for the more abundant noble metals. For Ir and Ru, which had to be analyzed from a minor line, the accuracy is much lower. Atomic ratios were calculated from intensity ratios by using Scofield interaction cross sections[9] together with an empirical response function of the spectrometer sensitivity to the photoelectron kinetic energy.

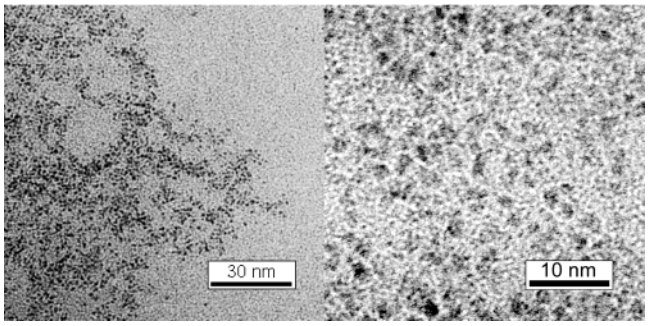

Figure 1. High-resolution TEM images of the 3−12-SB-stabilized colloid Pt(27)/Ru(20)/Os(23)/Ir(30)O_x at different magnification.

XRD(WAXS) Measurements. A Guinier diffractometer (Fa. Huber) was used. The instrument makes use of a Cu $K\alpha_1$ primary beam which is generated by a Johanson-type (111) germanium crystal. The diffractograms were recorded with a 45° transmission geometry.

Preparation and Characterization

Previous work had shown that the nature of the R-group in the betaine stabilizer $R(CH_3)_2N^+(CH_2)_3SO_3^-$ (or $R(CH_3)_2N^+(CH_2)_3CO_2^-$) is crucial to the success of the synthetic method.[3,4] If it is too short (e.g., R = *n*-butyl), precipitation of bulk metal oxide occurs. On the other hand, if it is too long (e.g., $R = C_{20}H_{43}$), water solubility is lost. In the present study, the betaine $C_{12}H_{25}(CH_3)_2N^+(CH_2)_3SO_3^-$ (3−12-SB**)** was used as the stabilizer. Upon adding aqueous solutions of H_2PtCl_6, $RuCl_3$, $OsCl_3$, and H_2IrCl_6 to a mixture of the stabilizer and a base such as Li_2CO_3 and heating the resulting mixture at 60 °C, the desired colloidal mixed metal oxides were formed with essentially quantitative conversion. Appreciable amounts of undesired precipitation of bulk metal oxide(s) were not observed. In all cases stable black colloidal solutions formed. Following dialysis freeze-drying (lyophilization) provided solid materials which can be redispersed in water. Several samples were prepared differing in the relative composition of the metals.

The initial experiments focused on the use of 1:1:1:1 amounts of the four salts, and indeed, a colloid was obtained displaying a Pt/Ru/Os/Ir ratio of 27/20/23/30 as evidenced by elemental analysis. TEM analysis shows the average size to be 1.3 ± 0.4 nm. To prepare the mixed metal oxide analogue of the Smotkin/Mallouk material, the relative amounts of the starting metal salts were adjusted to 44/41/10/5. Gratifyingly, a similar material resulted having a composition of Pt(40)/Ru(41)/Os(16)/Ir(3) and a size of 1.6 ± 0.3 nm, as shown by TEM analysis. Working at a 2-fold higher concentration resulted in similar material Pt(44)/Ru(41)/Os(11)/Ir(4) ($d_{TEM} = 1.2 \pm 0.3$), which demonstrates that absolutely identical conditions are not necessary for adequate reproducibility.

The high-resolution TEM images of the samples are all rather similar. Typical TEM images of the Pt(27)/Ru(20)/Os(23)/Ir(30) sample are shown in Figure 1. At high magnification, lattice planes can be seen (Figure 1b), which demonstrates the nanocrystalline nature of the material. Application of energy-dispersive X-ray analysis (EDX) proved the presence of all four metals, although a quantitative analysis was not possible due to partial overlap of peaks (e.g., the L_{21}-transition of osmium overlaps with the peaks due to copper present in the TEM grid).

To shed light on the electronic nature of the mixed metal oxide, e.g., the oxidation state of the metals therein, X-ray

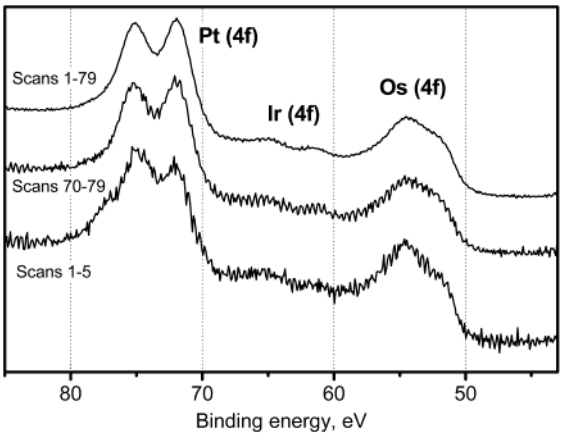

Figure 2. Development of Pt (4f), Ir (4f), and Os (4f) region of XP spectra during data acquisition [sample: the mixed metal oxide comprising Pt(40)/Ru(41)/Os(16)/Ir(3)].

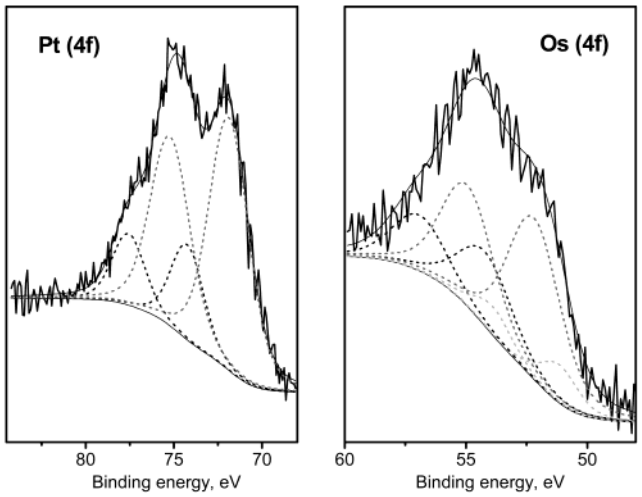

Figure 3. Analysis of the spectral shapes of the Pt (4f) and the Os (4f) signals [sample: the mixed metal oxide comprising Pt(40)/Ru(41)/Os(16)/Ir(3)]. For numerical results, see Table 1.

TABLE 1: XPS Binding Energies and Elemental Concentrations (Relative to C)

	Pt ($4f_{5/2}$)		Ir ($4f_{5/2}$)	Ru ($3p_{3/2}$)	Os ($4f_{5/2}$)		
BE	71.9	74.2	61.2	463.0	51.1	52.2	54.2
%	76	24	100	100	10	60	30
Me/C atomic ratio	0.008		0.0003	0.004	0.0020		

photoelectron spectroscopy (XPS) was applied. Due to the presence of excess stabilizer, which leads to carbon/metal ratios of > 70 (see Table 1), long data acquisition times were necessary. To document changes occurring with the samples during the measurements, intermediate results were saved and analyzed separately. Figure 2 shows typical results obtained in the case of the Pt(40)/Ru(41)/Os(16)/Ir(3) sample. It is obvious that the signal shapes of Pt and Os change significantly during data acquisition. Changes were also found with the stabilizer (N, S, O lines), but usually not with the Ru and Ir lines.[4]

Figure 3 shows the analysis of the spectra shapes of the Pt 4f and the Os 4f signals. In the case of Pt, binding energy and fwhm (full width at half-maximum) data can be unambiguously derived from the respective signals, while this is not possible for the Os region. For the latter, ambiguity was reduced by the fact that an extended set of spectra could be analyzed using Os states of the same binding energies within certain error margins (±0.2 eV).[4] In contrast to Pt and Os, the Ir and Ru signals indicate a single oxidation state. In fact, for the present sample, this could not be derived from the spectra after short acquisition time, but instead from the final spectra due to the invariability of Ir and Ru states observed with other metal oxide colloids.[4]

The Pt binding energies found indicate the presence of Pt(II) and Pt(IV) species. This was expected on the basis of our previous experience with Pt/Ru mixed metal oxides in which platinum occurs as Pt(II) and Pt(IV).[3a] Indeed, the redox properties of the two metals predict oxidation of ruthenium by platinum according to the following stoichiometry:

$$Pt^{4+} + 2\ Ru^{3+} \rightarrow Pt^{2+} + 2\ Ru^{4+}$$

This means that if in the synthesis the salts are chosen in a 1:1 proportion, some of the platinum will remain in the +4 oxidation state. The peak with the binding energy of 71.9 eV is assigned to hydroxy-platinum species of the type $Pt(OH)_2$ by comparison with reference data (72.3 eV, recalibrated).[10] The peak at ca. 74.2 eV is more difficult to assign because bulk PtO_2 and $Pt(OH)_4$ have similar Pt binding energies (74.7 and 74.3 eV, respectively).[10] It may well be that in the mixed metal oxide both Pt(IV) oxide and hydroxide species are present, but the fact that reduction during data acquisition leads to Pt(II) hydroxide species favors Pt(IV) hydroxide.

For the other metals, the binding energies found agree with those of bulk oxides (IrO_2, 61.7−62.0 eV; OsO_2, 51.7−52.0 eV;[10] RuO_2, 462.7[11] and 463.6 eV[12]), but the presence of hydroxide cannot be ruled out due to the lack of reference data. Analogously, the remaining Os states are difficult to assign. The minor species with a rather low binding energy of 51.1 eV (Os metal, 50.7 eV) seems to be insignificant in the analysis of the present material. It was, however, clearly established in other related multimetal oxide colloids such as $PtRuOsO_x$ prepared by the same method.[4] From the bulk composition, the elemental ratios between Pt, Ru, Os, and Ir are roughly 1:1:0.4:0.1, while a ratio of 1:0.5:0.25:0.04 was obtained by surface analysis. Obviously, there is a surface enrichment in platinum while the relation between the remaining elements equals the bulk relations within the experimental error. The XPS binding energies and elemental amounts relative to carbon are listed in Table 1.

We also wanted to apply X-ray diffractometry (XRD) to the samples in order to gain more insight in such properties as type of structure and size as well as size distribution of the nanoparticles. Specifically, X-ray wide-angle scattering (WAXS), which has been shown to be a powerful technique in the characterization of nanoparticles,[1k,13] was used. This method provides valuable structural information even though the material may be "X-ray amorphous". In doing so, a special software developed to simulate the diffraction of nanomatter, called Debye Function Analysis (DFA), was employed.[13] Basically DFA uses a linear combination of the Debye functions calculated for a set of particles of increasing size, as, for instance, closed-shell cuboctahedra with 13, 55, 147, 309, 561, 923, ... atoms. Noncrystallographic so-called multiply twinned particles (MTPs) can be employed likewise. The number fractions are used as free parameters, as well as the interatomic distance, which is a sensitive parameter of the simulation. The quality of the results depends strongly on the accuracy of the experiment. The method affords a careful measurement and subtraction of all background scattering contributions and usually requires the possibility to perform in situ experiments.[13c,d]

Some simplifications are unavoidable in such complex systems containing up to four metals. Here we use average scattering amplitude for all elements, which is equivalent to assuming a perfect alloying within the particles. In a previous

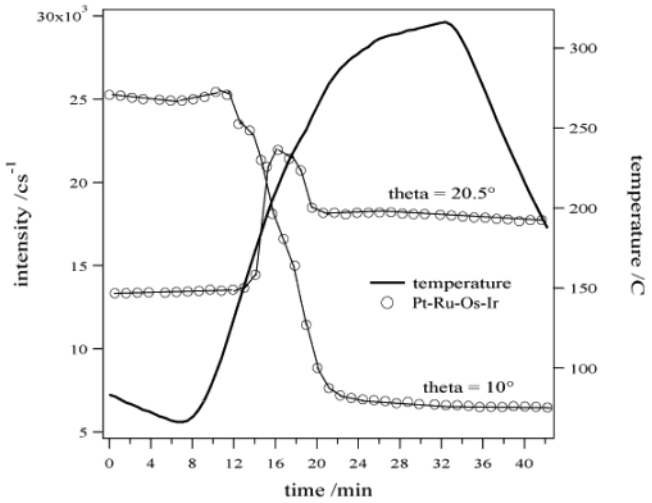

Figure 4. XRD(WAXS) results using sample Pt(27)/Ru(20)/Os(23)/Ir(30)O_x. Peak intensity measurement with an open receiving slit (8 mm) at the Bragg angles $\theta = 10°$ (3−12-SB-peak) and $\theta = 20.5°$ (strongest metal peak). The "as prepared" sample (circles) is studied in situ as a function of time and temperature (solid line) in a vacuum.

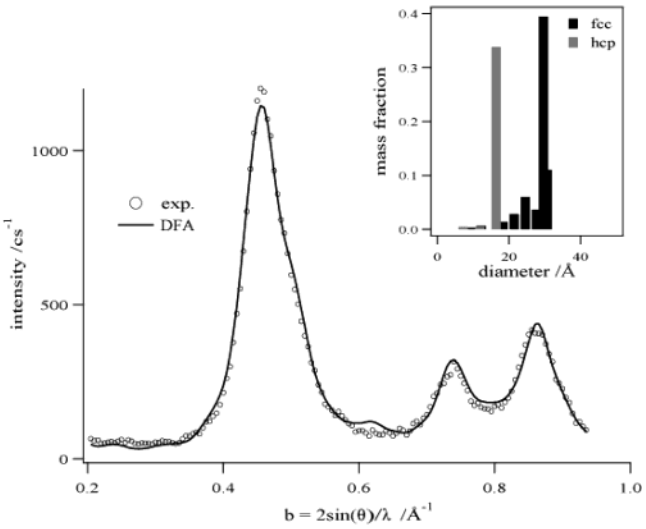

Figure 5. XRD(WAXS) results using sample Pt(27)/Ru(20)/Os(23)/Ir(30)O_x. Diffraction pattern after vacuum pyrolysis at 520°C, plotted vs the reciprocal scattering length $b = 2 \sin(\theta)/\lambda$. The pattern is corrected for the 3−12-SB background and overlapping narrow peaks produced by two 0.1 mm of beryllium plates that sandwich the colloidal material and subjected to the usual angular correction factors (absorption, polarization, geometric factor). The solid line represents a DFA simulation with a combination of hcp model particles and twinned fcc particles. The mass fractions in the individual particles used for DFA are plotted vs their sphere-equivalent diameters at the insert of the figure.

study of the two-component colloid system Pt−Ru, it was shown that this is a reasonable assumption.[13d] In fact the elements Pt, Ir, and Os are nearly indistinguishable by X-rays.

In the present study, analysis of the mixed metal oxide itself was not feasible due to the presence of the organic stabilizer (3−12-SB) which contributes a multitude of crystalline reflections superimposed on the scattering of the metal fraction. We therefore performed an in situ pretreatment by a vacuum pyrolysis (or ex situ under argon) of the samples at around 300 °C, which fully reduces the particles to the metal state without significant particle growth.[4] This causes partial destruction of 3−12-SB, its contribution becoming amorphous and less strong. Only one diffuse halo is observed in the low-angle region, which makes background correction very easy. Figure 4 shows the time-dependent variations of the intensity around a strong 3−12-SB-peak ($\theta = 10°$), and around the strong metal phase peak expected at $\theta = 20.5°$ for Pt−Ru−Os−Ir (27/20/23/30).[14] The temperature is ramped between room temperature and 320 °C. The break-down of the 3−12-SB structure begins at ∼150 °C, and the metal peak emerges time-correlated. Full reduction is reached at ∼250 °C, with no further increase of the peak intensity. Such an increase would be related to a growth of the primarily formed particles.

It turns out that the Pt(27)/Ru(20)/Os(23)/Ir(30) material following the heat treatment described above is best characterized as consisting of a fraction of fcc particles (60% by mass) and hcp particles (40%). A major improvement of the fit is gained by adding stacking faults in the model. Figure 5 shows the corrected diffraction pattern of the alloy compared with that of the calculated fcc/hcp simulation (solid line) after vacuum annealing to 520 °C. The insert shows the mass fractions versus sphere equivalent diameters of the model particles. The average size is around 2 nm.

The most likely explanation for the existence of hcp particles is a certain phase segregation of the bulk hcp elements Os and Ru. Osmium in the bulk phase is only soluble to 25 mol % in platinum. Ruthenium is soluble to 50 mol %, but according to its low Z, it adds not much to the total intensity, which is proportional to Z^2. Annealing at high temperature seems to promote this effect, since at 520 °C the phase separation is more evident than at 320 °C. The size histogram in Figure 5 gives a clear separation in the sizes, the smaller being the hcp particles. Simulations with fcc and decahedra also end at comparable R-values but do not describe some specific features at the high angle diffraction peaks.[4]

The question arises as to whether DFA is able to distinguish between complete alloying and a physical mixture of particles, each of those being composed of one element. We have calculated the hypothetical diffraction pattern of an equimolar mixture of particles of the four elements, each with the same size (334 atoms), but maintaining their bulk structure and interatomic spacings. According to our calculations, such a situation can definitely be excluded.

Finally, Pt(44)/Ru(41)/Os(11)/Ir(4) colloid was studied, which is close to the optimum composition found by Smotkin and Mallouk for use in fuel cell application.[5] We performed an ex situ pretreatment in argon for simplicity, since the reduction behavior was already known from previous experiments. In contrast to the equimolar material, the best fit in this case was achieved with a combination of decahedral and larger fcc-type model particles. The corresponding DFA simulation of Pt−Ru−Os−Ir(44/41/11/4) after heating to maximal 310 °C in Ar is shown in Figure 6. The fit is nearly perfect with a mean deviation of less than 0.4% from the experiment. Simulations with fcc/hcp model particles definitely failed, the R-factor being reduced by a factor of 2. The two panels at the bottom of Figure 6 display the size distribution of the model particles weighted by their mass (left panel) and by their number (right panel), respectively. Note the differences, since larger particles appear with a $\sim R^3$ larger fraction if weighted by mass. Note also that the weight parameters for individual particles in the panels are afflicted with large errors, but the assembly as whole can be transformed to a more realistic smooth distribution.[13a] The majority fraction is found to be the decahedral particles (70 wt %), which are also smaller in size. The 30 wt % of twinned fcc particles are located around 3.5 nm (about 1450 atoms). The high quality of this fit allows also a rather accurate determination of "lattice constants" for the two individual particle systems,[13e]

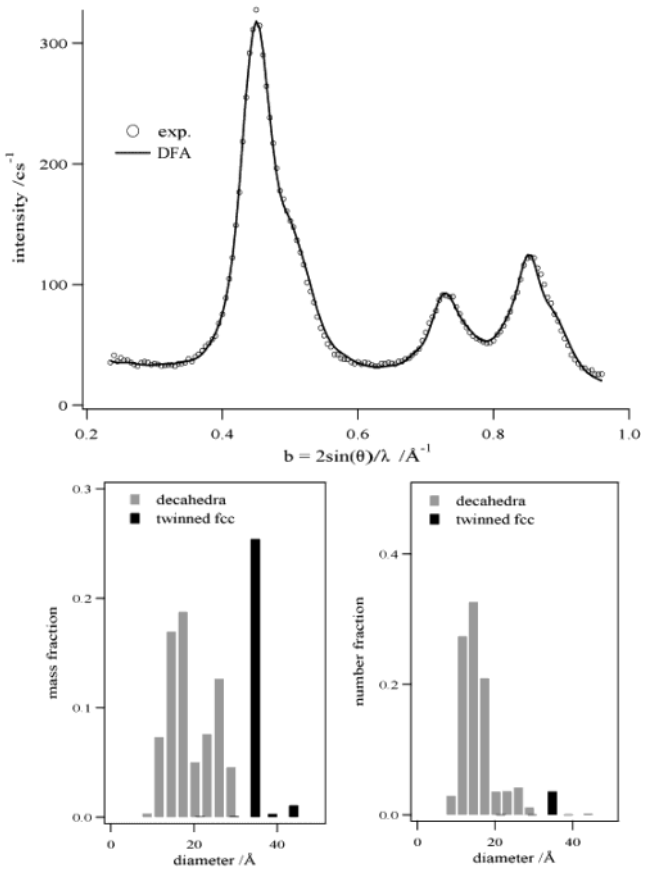

Figure 6. XRD(WAXS) results using sample Pt(44)/Ru(41)/Os(10)/Ir(5)O_x. Diffraction pattern after previous pyrolysis in Ar at maximal 320 °C. The solid line represents a DFA simulation with a combination of decahedral model particles and twinned fcc particles. The panels at the bottom show the fractions weighted by mass and weighted by number, respectively, for the individual particles used for DFA.

related to that of bulk platinum: the fcc-particles are "contracted" by 0.8% ± 0.2%, and the decahedral particles are contracted by 2.0% ± 0.2%. The difference is relevant, and can be explained by some enrichment of the smaller sized atoms of osmium and ruthenium in decahedral particles. Although this appears to be rather speculative, it might be of relevance in the extraordinary catalytic performance of this quaternary system (see below).

Immobilization and Use as Electrocatalyst. To be able to test the electrocatalytic properties of the tetrametal oxide colloid $PtRuOsIrO_x$ having a metal ratio of 42/44/9/5, it was necessary to support it on high surface conducting carbon (e.g., Vulcan XC 72). Previous experience had shown that immobilization of metal oxide colloids on supports of this kind is less straightforward than in the case of the corresponding metal colloids in the zerovalent form.[3] For example, the transformation of 3−12-SB-stabilized colloidal $PtRuO_x$ into the corresponding Pt/Ru colloid was easily executed by treatment with H_2 (1 bar) in water at room temperature for 24 h,[3] and immobilization on Vulcan XC 72 posed no problems.[4] In the present case, this procedure also resulted in smooth reduction. The aqueous solution was then buffered with citrate (pH 3.5) and used in the immobilization.[4] The immobilizate (15% metal content), having a final particle size of 2.3 ± 0.5 nm was then incorporated in a conventional membrane-electrode-assembly (MEA) which is part of the PEFC. This material as well as the previously prepared Pt/Ru-Vulcan[4] and the usual commercial E-TEK Pt/Ru-Vulcan (which is normally employed in experiments of this kind) were first tested in hydrogen oxidation in the absence of CO. The current voltage curves are shown in Figure 7. It is evident that the Pt/Ru/Os/Ir catalyst and the commercial catalyst show similar performance. However, if the electrocatalytic experiments are performed in the presence of varying amounts of CO, the catalysts behave differently. Upon applying 50 ppm CO (or more), the performance of the commercial catalyst is reduced drastically. In sharp contrast, the catalytic profile of the Pt/Ru/Os/Ir catalyst is different (Figure 7). It shows a significantly improved tolerance toward CO. At 50 ppm CO contamination and at a voltage of 0.4 V, electrical performance is about 50% higher with the Pt/Ru/Os/Ir catalyst than with the commercial E-TEK Pt/Ru−Vulcan system. Even at 1039 ppm CO the fuel cell still displays appreciable performance.[4] Thus, the results of Smotkin and Mallouk concerning the Pt/Ru/Os/Ir combination using different synthetic methods[5] are substantiated.

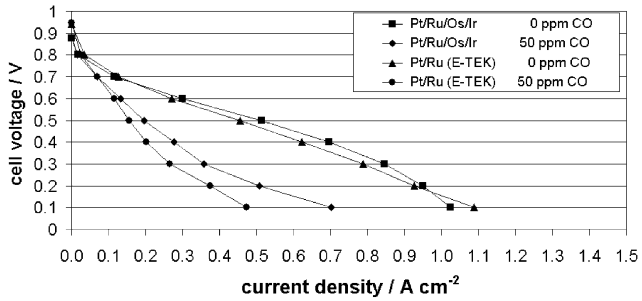

Figure 7. Current−potential curves of PEFC single cells under ambient pressure operation with H_2/air and H_2 , 50 ppm CO/air; T = 80°C; active area = 17.4 cm^2. Anode: Pt(42)/Ru(44)/Os(9)/Ir(5) catalyst supported on Vulcan XC 72 (0.20 mg/cm^2) and commercial PtRu-ETEK supported on Vulcan XC 72 (0.20 mg/cm^2). Cathode: commercial E-TEK electrode (0.5 mg/cm^2 Pt).

Conclusions

Our previously described method for the preparation of water-soluble colloidal transition metal oxides such as PtO_2 and $PtRuO_x$ can be extended successfully to the synthesis of the unusual mixed metal oxide $PtRuOsIrO_x$ incorporating four different metals. Accordingly, appropriate metal salts are hydrolyzed under basic conditions in the presence of the betain-stabilizer $C_{12}H_{25}(CH_3)_2N^+(CH_2)_3SO_3^-$, leading to nanoparticles in the size range of 1.2−1.6 nm, which were characterized by elemental analysis, TEM and XPS. Accordingly, metal oxide and metal hydroxide structural units as well as mixed valent species are present. Vacuum pyrolysis at 300−320 °C leads to the reduction of the solid material with formation of nanoparticles comprising Pt, Ru, Os, and Ir in the metallic form, which were characterized by XRD-DFA. Colloidal solutions of aqueous $PtRuOsIrO_x$ can be reduced with hydrogen at room temperature with formation of aqueous solutions of the corresponding 3−12-SB-stabilized PtRuOsIr colloids. The latter are readily immobilized on high surface conducting carbon (Vulcan), resulting in materials which can be incorporated in fuel cells (PEFCs). These electrocatalysts, which are of the Smotkin/Mallouk type, are more efficient than commercial Pt/Ru-based catalysts because they show an unusually high resistance to CO poisoning.

Acknowledgment. We thank the Land NRW (NaKaB) and the Fonds der Chemischen Industrie for financial support and B. Tesche and B. Spliethoff for the TEM analyses.

References and Notes

(1) See, for example: (a) In *Nanoparticles and Nanostructured Films*; Fendler, J. H., Ed.; Wiley-VCH: Weinheim, 1998. (b) In *Clusters and*

Colloids: From Theory to Applications; Schmid, G., Ed.; VCH: Weinheim, 1994. (c) Pileni, M. P. *Ber. Bunsen-Ges.* **1997**, *101*, 1578. (d) Ahmadi, T. S.; Wang, Z. L.; Green, T. C.; Henglein, A.; El-Sayed, M. A. *Science* **1996**, *272*, 1924. (e) De Caro, D.; Bradley, J. S. *Langmuir* **1997**, *13*, 3067. (f) Ely, T. O.; Amiens, C.; Chaudret, B.; Snoeck, E.; Verelst, M.; Respaud, M.; Broto, J.-M. *Chem. Mater.* **1999**, *11*, 526. (g) Watzky, M. A.; Finke, R. G. *J. Am. Chem. Soc.* **1997**, *119*, 10382. (h) Bönnemann, H.; Brijoux, W.; Brinkmann, R.; Dinjus, E.; Joussen, T.; Korall, B. *Angew. Chem.* **1991**, *103*, 1344; *Angew. Chem., Int. Ed. Engl.* **1991**, *30*, 1312. (i) Mulvaney, P.; Giersig, M. *J. Chem. Soc., Faraday Trans.* **1996**, *92*, 3137. (j) Reetz, M. T.; Maase, M. *Adv. Mater.* **1999**, *11*, 773. (k) Reetz, M. T.; Winter, M.; Breinbauer, R.; Thurn-Albrecht, T.; Vogel, W. *Chem. Eur. J.* **2001**, *7*, 1084.

(2) See, for example: (a) Lume-Pereira, C.; Baral, S.; Henglein, A.; Janata, E. *J. Phys. Chem.* **1985**, *89*, 5772. (b) Harriman, A.; Thomas, J. M.; Millward, G. R. *New J. Chem.* **1987**, *11*, 757. (c) Kalyanasundaram, K.; Grätzel, M. *Angew. Chem.* **1979**, *91*, 759; *Angew. Chem., Int. Ed. Engl.* **1979**, *18*, 701. (d) Christensen, P. A.; Harriman, A.; Porter, G.; Neta, P. *J. Chem. Soc., Faraday Trans. 2* **1984**, *80*, 1451. (e) Claerbout, A.; Nagy, J. B. Preparation of Monodisperse Colloidal Platinum-Rhenium Dioxide Particles Using Microemulsions. In *Preparation of Catalysts V*; Poncelet, G., Ed.; Elsevier: Amsterdam, 1991; Vol. 63; p 705. (f) Pileni, M. P. *Langmuir* **1997**, *13*, 3266. (g) Reetz, M. T.; Quaiser, S. A.; Winter, M.; Becker, J. A.; Schäfer, R.; Stimming, U.; Marmann, A.; Vogel, R.; Konno, T. *Angew. Chem.* **1996**, *108*, 2228; *Angew. Chem., Int. Ed. Engl.* **1996**, *35*, 2092. (h) Nayak, S. K.; Jena, P. *J. Am. Chem. Soc.* **1999**, *121*, 644. (i) Li, J.; Wang, Y. J.; Zou, B. S.; Wu, X. C.; Lin, J. G.; Guo, L.; Li, Q. S. *Appl. Phys. Lett.* **1997**, *70*, 3047. (j) Zhiwen, C.; Shuyuan, Z.; Shun, T.; Fanqing, L.; Jian, W.; Sizhao, J.; Yuheng, Z. *J. Cryst. Growth* **1997**, *180*, 280. (k) Kodama, R. H.; Makhlouf, S. A.; Berkowitz, A. E. *Phys. Rev. Lett.* **1997**, *79*, 1393. (l) Lee, G. H.; Huh, S. H.; Jeong, J. W.; Choi, B. J.; Kim, S. H.; Ri, H.-C. *J. Am. Chem. Soc.* **2002**, *124*, 12094. (m) Feldmann, C.; Jungk, H.-O. *Angew. Chem.* **2001**, *113*, 372; *Angew. Chem., Int. Ed.* **2001**, *40*, 359. (n) Herrig, H.; Hempelmann, R. *Mater. Lett.* **1996**, *27*, 287. (o) Weller, H. *Angew. Chem.* **1993**, *105*, 43; *Angew. Chem., Int. Ed. Engl.* **1993**, *32*, 41. (p) Yang, J.; Mei, S.; Ferreira, J. M. F. *J. Am. Ceram. Soc.* **2000**, *83*, 1417.

(3) (a) Reetz, M. T.; Koch, M. G. *J. Am. Chem. Soc.* **1999**, *121*, 7933. (b) Reetz, M. T.; Koch, M. G. Patent application DE-A 19852547.8, 13.11.1998. (c) Koch, M. G. Dissertation, Ruhr-Universität Bochum, Bochum, Germany, 1999.

(4) Lopez, M. Dissertation, Ruhr-Universität Bochum, Bochum, Germany, 2002.

(5) Reddington, E.; Sapienza, A.; Gurau, B.; Viswanathan, R.; Sarangapani, S.; Smotkin, E. S.; Mallouk, T. E. *Science* **1998**, *280*, 1735.

(6) Gurau, B.; Viswanathan, R.; Liu, R.; Lafrenz, T. J.; Ley, K. L.; Smotkin, E. S. *J. Phys. Chem. B* **1998**, *102*, 9997.

(7) Boyen, H.-G. *"MacFit", Surface Analysis Software Package*; University of Basel: Basel, Switzerland.

(8) Wark, M.; Koch, M.; Brückner, A.; Grünert, W.*J. Chem. Soc., Faraday Trans.* **1998**, 2033.

(9) Scofield, J. H. *J. Electron Spectrosc. Relat. Phenom.* **1976**, *8*, 129.

(10) (a) Burkhardt, J.; Schmidt, L. D. *J. Catal.* **1989**, *116*, 240. (b) Roth, C.; Goetz, M.; Fuess, H. *J. Appl. Electrochem.* **2001**, *31*, 793. (c) Wagner, D. In *Practical Surface Analysis*, 2nd ed.; Briggs, D. Seah, M. P., Eds.; Wiley: Chichester, 1990; Vol. 1, Appendix 5.

(11) Lenarda, M.; Storaro, L.; Ganzerla, R.; Bertoncelli, R. *J. Mol. Catal. A: Chem.* **1999**, *144*, 151.

(12) Latham, K.; Thompsett, T.; Williams, C. D.; Round, C. I. *J. Mater. Chem.* **2000**, *10*, 1235

(13) (a) Gnutzmann, V.; Vogel, W. *J. Phys. Chem.* **1990**, *94*, 4991. (b) Vogel, W.; Rosner, B.; Tesche, B. *J. Phys. Chem.* **1993**, *97*, 11611. (c) Hartmann, N.; Imbihl, R.; Vogel, W. *Catal. Lett.* **1994**, *28*, 373. (d) Vogel, W.; Britz, P.; Bönnemann, H.; Rothe, J.; Hormes, J. *J. Phys. Chem. B* **1997**, *101*, 11029. (e) Vogel, W.; Bradley, J. S.; Vollmer, O.; Abraham, I. *J. Phys. Chem. B* **1998**, *102*, 10853. (f) Vogel, W. *Cryst. Res. Technol.* **1998**, *33*, 1141. (g) Dassenoy, F.; Vogel, W.; Alonso-Vante, N. *J. Phys. Chem. B*, in press.

(14) In a preview study,[4] the 3−12-SB-stabilized trimetal oxide PtRuO-sO$_x$ (d_{TEM} = 1.3 nm) was prepared by the same general procedure and also studied by WAXS.